

Rising Multi-Armed Bandits with Known Horizons

Seockbean Song¹ Chenyu Gan² Youngsik Yoon³ Siwei Wang⁴ Wei Chen⁴ Jungseul Ok^{1,3,†}

Abstract

The Rising Multi-Armed Bandit (RMAB) framework models environments where expected rewards of arms increase with plays, which models practical scenarios where performance of each option improves with the repeated usage, such as in robotics and hyperparameter tuning. For instance, in hyperparameter tuning, the validation accuracy of a model configuration (arm) typically increases with each training epoch. A defining characteristic of RMAB is *horizon-dependent optimality*: unlike standard settings, the optimal strategy here shifts dramatically depending on the available budget T . This implies that knowledge of T yields significantly greater utility in RMAB, empowering the learner to align its decision-making with this shifting optimality. However, the horizon-aware setting remains underexplored. To address this, we propose a novel CUMulative Reward Estimation UCB (CURE-UCB) that explicitly integrates the horizon. We provide a rigorous analysis establishing a new regret upper bound and prove that our method strictly outperforms horizon-agnostic strategies in structured environments like “linear-then-flat” instances. Extensive experiments demonstrate its significant superiority over baselines.

1. Introduction

Unlike standard Multi-Armed Bandit (MAB) problems where rewards remain constant, the Rising Multi-Armed Bandit (RMAB) framework models environments where performance improves with repeated usage, mirroring the intuitive process of gaining proficiency. However, while often analyzed theoretically under indefinite horizons, practical applications are typically governed by strict, finite resource limits.

[†]Corresponding author ¹Graduate School of AI, POSTECH, Pohang, Republic of Korea ²IIIS, Tsinghua University, Beijing, China ³Department of CSE, POSTECH, Pohang, Republic of Korea ⁴Microsoft Research, Beijing, China. Correspondence to: Jungseul Ok <jungseul.ok@postech.ac.kr>.

Preprint. February 12, 2026.

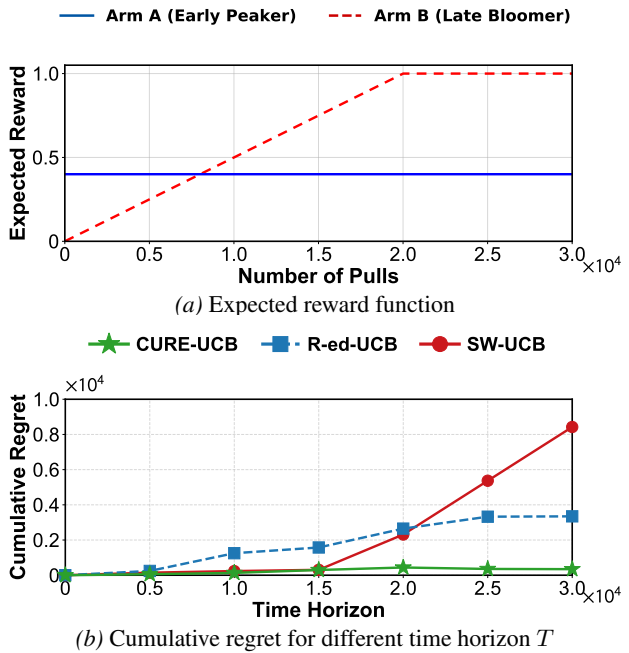


Figure 1. Demonstration of Horizon-Adaptiveness. (a) Expected reward functions. The **Arm A** represents an *Early Peaker* (high initial reward, limited growth), and the **Arm B** represents a *Late Bloomer* (low initial reward, high potential). (b) Cumulative regret results across varying time horizons T . **CURE-UCB** (Ours) consistently achieves small regret across all horizons. In contrast, baselines suffer structural failures. **R-ed-UCB** (horizon-agnostic rising bandit algorithm) incurs high regret in short horizons ($T=10,000$) whereas **SW-UCB** (non-stationary bandit algorithm) fails in long horizons ($T=30,000$).

Key applications of RMAB include hyperparameter tuning in Automated Machine Learning (Li et al., 2018; 2020) and robotics, particularly within hierarchical reinforcement learning (Song et al., 2024; Yoon et al., 2024). In these applications, the performance of a selected option (a training configuration or a robotic sub-skill) improves with repeated execution. Crucially, these practical domains typically operate under a known, finite horizon (e.g., GPU hours) provided to the learner. This explicit knowledge offers a significant advantage, enabling the deployment of a horizon-adaptive strategy that maximizes efficiency by dynamically shifting its priority, exploiting options with immediate gain when the horizon is limited versus investing in options with high potential when the remaining horizon is sufficient.

Figure 1 demonstrates the strategic utility gained by explicitly leveraging this known horizon. In this setting, the optimal policy allocates every resource to the early peaker arm for short horizon, whereas it shifts its focus to the late bloomer arm when the horizon is sufficiently large (e.g., $T > 15000$). R-ed-UCB, designed as a horizon-agnostic rising bandit algorithm, estimates future rewards based on growth rates. Initially, it selects the early peaker arm due to its superior immediate rewards. However, as the estimated potential of the late bloomer arm increases, the algorithm tends to switch to the late bloomer even when the remaining horizon is insufficient to recover the initial performance deficit. Consequently, it suffers from significant regret in short-horizon settings where the optimal policy dictates sticking to the early peaker ($T \approx 10000$). SW-UCB, a non-stationary algorithm, estimates the instantaneous mean using a sliding window. It does not account for the cumulative growth potential. As a result, it fails to switch to the late bloomer arm even when the horizon is sufficiently large, leading to linear regret as it continues to select the suboptimal early peaker ($T \approx 50000$).

In contrast, our proposed CUMulative Reward Estimation UCB (CURE-UCB) efficiently adapts its strategy by explicitly leveraging the known horizon T . By estimating the cumulative reward each arm would yield over the entire remaining duration, CURE-UCB naturally identifies the horizon-dependent switching point. This enables CURE-UCB to align with the optimal policy: prioritizing investment in the late bloomer’s growth when the remaining horizon permits, while shifting to the early peaker’s immediate returns as the horizon shortens.

We further provide a rigorous theoretical analysis validating the structural advantages of horizon awareness in RMAB. Specifically, in structured environments, we demonstrate a strict dominance result (Theorem 5.2) by showing that CURE-UCB systematically avoids the wasteful exploration of saturated arms compared to horizon-agnostic baselines. Extending beyond these structured settings, we derive a general regret upper bound (Theorem 5.4), guaranteeing the efficiency of CURE-UCB across broad concave rising environments.

We validate our theoretical findings through extensive experiments encompassing diverse synthetic environments to test robustness across various reward growth patterns. Crucially, we demonstrate practical applicability in a real-world online model selection task, confirming that CURE-UCB consistently outperforms variant of baselines in both controlled and practical settings.

Our main contributions are summarized as follows:

- We revisit the concept of horizon-dependent optimality within the RMAB framework, highlighting its crucial role in finite-horizon settings in Section 3.

- We propose CURE-UCB, a horizon-aware algorithm that estimates the bounded cumulative potential, ensuring alignment with the horizon-dependent optimality in Section 4.
- We establish a strict dominance result over agnostic strategies in structured environments (Theorem 5.2) and regret upper bound of CURE-UCB in general cases (Theorem 5.4) in Section 5.
- We empirically validate our method’s superiority across diverse synthetic benchmarks and a practical online model selection task, demonstrating its ability to capture high-potential arms missed by baselines in Section 6.

2. Related works

The RMAB framework can be viewed as a specific instance of non-stationary bandits (Besbes et al., 2014; Allesiardo et al., 2017), specifically the rested setting where rewards evolve solely based on the number of pulls. However, standard non-stationary strategies relying on forgetting mechanisms(Garivier & Moulines, 2011; Trovo et al., 2020) or periodic restarts(Allesiardo et al., 2017; Besbes et al., 2014) are ill-suited for this context. As they are designed to track the current mean rather than predict future growth, they fail to capture the rising trend essential for optimal decision-making.

To leverage the inherent structure of reward dynamics, recent literature (Heidari et al., 2016; Metelli et al., 2022; Fiandri et al., 2024; Xia et al., 2024; Amichay & Mansour, 2025; Fiandri et al., 2025) has focused on environments with rising trends . Heidari et al. (2016) established the foundational framework for the rested RMAB, introducing the notion of policy regret to compare the learner against an optimal dynamic policy. In the stochastic setting, several prominent strategies operate in a horizon-agnostic manner, primarily focusing on tracking instantaneous means or growth rates. Specifically, Metelli et al. (2022) introduced R-ed-UCB, which utilizes a derivative-based estimator to capture growth rates, providing $\tilde{O}(T^{2/3})$ theoretical guarantees for concave rising functions under some conditions. Fiandri et al. (2024) introduced ET-SWGTS, adapting Thompson Sampling to the RMAB setting by employing an initial forced exploration phase to prevent the starvation of potential high-growth arms, combined with a sliding-window mechanism to handle non-stationarity. Xia et al. (2024) developed TI-UCB to detect convergence points in increasing-then-converging scenarios. While these strategies offer robust performance, they remain predominantly horizon-agnostic, directing their focus toward tracking instantaneous means or growth rates. Distinct from these approaches, (Amichay & Mansour, 2025) recently proposed R-ed-AE, a horizon-aware algorithm. However, their method

relies on a successive elimination strategy specifically tailored for linear drifts. This distinguishes it from our work, which employs a UCB-based framework designed to handle a broader class of problem instances beyond linear settings.

3. Problem Formulation

We consider the Rising Multi-Armed Bandit (RMAB) problem, where the expected reward of each arm increases with the number of times it has been played. Let K be the number of arms, indexed by $[K] := \{1, \dots, K\}$. At each round $t \in [T]$, the learner selects an arm $I_t \in [K]$ and observes a reward X_t . This reward is drawn independently from a distribution $D_{I_t}(N_{I_t, t-1})$, where $N_{i, t-1}$ denotes the number of times arm i has been played up to time $t-1$.

We assume that the reward distribution $D_i(n)$ is σ^2 -subgaussian with a known variance parameter σ^2 . Let $\mu_i(n) := \mathbb{E}_{X \sim D_i(n)}[X]$ denote the expected reward of arm i on its n -th pull, assuming $\mu_i(n) \in [0, 1]$ for all $i \in [K]$ and $n \in [T]$. We denote the problem instance by the vector of mean reward functions $\mu := (\mu_1, \mu_2, \dots, \mu_K)$. A defining characteristic of the rising bandit setting is that the mean reward is non-decreasing for all arms $i \in [K]$ and number of plays $n \geq 1$:

$$\gamma_i(n) := \mu_i(n+1) - \mu_i(n) \geq 0. \quad (1)$$

The learner's history up to time t is denoted by $\mathcal{H}_t := \{(I_\tau, X_\tau) : \tau \in [t]\}$. A policy π maps this history \mathcal{H}_{t-1} to an arm $I_t \in [K]$ to be played at round t .

For analytical tractability, consistent with the rising bandit literature (Heidari et al., 2016; Metelli et al., 2022), we assume the concavity of the mean reward function μ_i . This implies that while the expected rewards increase, the marginal gain from each additional pull is non-increasing.

Assumption 3.1. (Concavity of μ_i) For each arm $i \in [K]$ and number of plays $n \geq 1$, the increments are non-increasing:

$$\gamma_i(n) \geq \gamma_i(n+1). \quad (2)$$

Regret Minimization The objective of the learner is to maximize the cumulative reward over a finite horizon T . Let $V(\pi, T) := \mathbb{E}_\pi \left[\sum_{t=1}^T X_t \right]$ be the expected cumulative reward of a policy π . We define the optimal policy π^* as the policy that maximizes the expected cumulative reward:

$$\pi^* := \arg \max_{\pi} V(\pi, T). \quad (3)$$

The performance of a policy π is measured by its regret, defined as the difference between the expected cumulative reward of the optimal policy and that of π :

$$Reg_\mu(\pi, T) := V(\pi^*, T) - V(\pi, T). \quad (4)$$

It is crucial to distinguish the regret definition employed here from that used in standard stochastic bandits. Standard algorithms typically optimize for external regret, comparing performance against a single best action fixed in hindsight. While widely used, this metric is conceptually inadequate for rested bandits where rewards are not suited for environments where rewards depend on the history of actions (Arora et al., 2012). Therefore, we adopt the notion of policy regret. This metric compares the learner against the optimal strategy π^* that maximizes the expected cumulative reward over the specific horizon T . As we establish in Proposition 3.2, in RMAB setting, this optimal strategy indeed reduces to selecting a single arm and playing it continuously, which is similar to the external regret benchmark. However, adopting the policy regret framework is essential to rigorously define optimality in an environment where rewards are driven by the accumulation of plays.

While identifying π^* generally involves dynamic planning, the non-decreasing reward structure simplifies the optimal strategy. Specifically, the optimal policy for given T reduces to selecting a single arm and playing it continuously (Heidari et al., 2016):

Proposition 3.2 (Structure of Optimal Policy). *For a rising bandit problem with a finite horizon T , the optimal policy π^* consists of selecting a single arm $i^* \in [K]$ and playing it for all $t \in T$. This arm i^* is determined by maximizing the cumulative reward over the horizon T :*

$$i^* = \arg \max_{i \in [K]} \sum_{t=1}^T \mu_i(t). \quad (5)$$

This structural property offers a crucial insight regarding the nature of decision-making. At any round $t > 1$, the optimization problem for the remaining horizon $T - t$ is structurally equivalent to a new RMAB instance with shifted reward functions. This implies that horizon-dependent optimality applies continuously at every step. An arm identified as optimal at the beginning may no longer be optimal for the remaining horizon $T - t$. Therefore, the optimal policy is defined as the one selecting the arm that maximizes the cumulative reward specifically over the remaining steps, conditioned on the current history. This insight directly motivates our proposed algorithm. We design CURE-UCB to explicitly estimate and maximize this bounded remaining cumulative potential to align with the shifting optimality condition.

3.1. Necessity of Horizon Awareness

To provide theoretical intuition on why horizon awareness is indispensable in RMAB, we analyze the two-armed example illustrated in Figure 1. Consider two arms with deterministic mean reward functions defined as $\mu_A(n) = 0.4$ (Early Peaker) and $\mu_B(n) = \min(1, \frac{n}{20000})$ (Late Bloomer)

According to Proposition 3.2, the optimal policy π^* is selecting single arm continuously to maximize cumulative reward. That is, it continuously pulls arm A for $T < 16,000$, while it shifts to arm B for $T > 16,000$.

Now, consider an arbitrary horizon-agnostic policy π . Since π is unaware of T , its action sequence at any time step t remains invariant regardless of the actual horizon T . Let N denote the number of times π selects arm 1 up to $t = 8,000$. We observe a fundamental performance inefficiencies:

- **Case 1 ($N < 4,000$):** The policy prioritizes the late bloomer prematurely. While this might be beneficial for very large T , it leads to significant regret in short-horizon settings (e.g., $T \approx 10,000$) where the optimal strategy is to stick with the early peaker.
- **Case 2 ($N > 4,000$):** The policy adheres to the early peaker too long. Although efficient for short horizons, it fails to sufficiently invest in the late bloomer's growth, resulting in substantial regret as T grows large (e.g., $T \approx 30,000$).

This objective mismatch reveals a fundamental inefficiencies inherent in horizon-agnostic strategies. Since such algorithms operate without knowledge of T , they are structurally incapable of adapting to the shifting optimal policy, making them prone to significant regret in either short or long horizons depending on their initial exploration bias. Consequently, a horizon-aware approach like CURE-UCB is required to explicitly leverage the remaining horizon, ensuring that every decision is consistently aligned with the true horizon-dependent optimality.

4. Algorithm

Algorithm 1 CURE-UCB

```

1: Input: Horizon  $T$ , Number of arms  $K$ 
2: Initialize: Play each arm  $i \in [K]$  twice.
3: for  $t = 2K + 1, \dots, T$  do
4:   Compute index  $B_i(t)$  for each arm, where  $B_i(t)$  is
      defined in equation 6
5:   Play arm  $I_t = \arg \max_{i \in [K]} B_i(t)$  and observe  $X_t$ .
6:   Update estimates and counter  $N_{I_t} \leftarrow N_{I_t} + 1$ .
7: end for

```

Motivated by the theoretical insight that the optimal strategy prioritizes the cumulative potential over the remaining horizon, we propose the CUMulative Reward Estimation UCB (CURE-UCB) algorithm. In contrast to conventional approaches that depend on instantaneous estimates, CURE-UCB explicitly estimates the aggregate future potential that each arm offers over the remaining horizon. This cumulative perspective enables CURE-UCB to adaptively align its strategy with the horizon-dependent optimality. The complete procedure is outlined in Algorithm 1.

4.1. The Horizon-Adaptive Index

The core of CURE-UCB is the construction of a horizon-adaptive index, denoted as $B_i(t)$. Unlike standard UCB indices that target instantaneous rewards, this index is designed to estimate the average expected reward that arm i would yield over the remaining horizon $(T - t)$, assuming it is selected continuously. The index is formally defined as the sum of three distinct components:

$$\begin{aligned}
 B_i(t) := & \underbrace{\frac{1}{h_i} \sum_{l=N_{i,t-1}-h_i+1}^{N_{i,t-1}} X_i(l)}_{\text{(i) Recent average}} \\
 & + \underbrace{\frac{(T-t)}{2} \cdot \frac{1}{h_i} \sum_{l=N_{i,t-1}-h_i+1}^{N_{i,t-1}} \frac{X_i(l) - X_i(l-h_i)}{h_i}}_{\text{(ii) Expected future cumulative gain}} \\
 & + \underbrace{\sigma \sqrt{\frac{2[3(T-t)^2 + 8h_i^2] \log t^3}{4h_i^3}}}_{\text{(iii) Exploration Bonus}}
 \end{aligned} \tag{6}$$

where σ is the standard deviation and h_i is the size of the sliding window governing a bias-variance tradeoff between employing few recent observations (less biased), compared to many past observations (less variance).

The components of $B_i(t)$ are interpreted as follows:

- (i) *Recent Average:* This term estimates the current instantaneous expected reward of arm i . It reflects the arm's performance at the current moment and serves as the starting point for estimating the bounded cumulative potential over the remaining horizon.
- (ii) *Estimated Average Future Gain:* This term captures the additional value expected from the arm's growth. Specifically, it represents the average increment in reward over the remaining duration $(T - t)$ if the arm's performance continues to rise linearly. Geometrically, this corresponds to the midpoint of the projected reward trajectory, effectively estimating the average height of the cumulative reward area shown in Figure 2.
- (iii) *Exploration Bonus:* This term accounts for uncertainty and encourages the exploration of arms that have not been played sufficiently often. The exploration bonus used here is intentionally larger than typical bonuses in UCB-based algorithms for stationary bandit settings, because CURE-UCB predicts future rewards in a rising setting, where uncertainty is inherently greater.

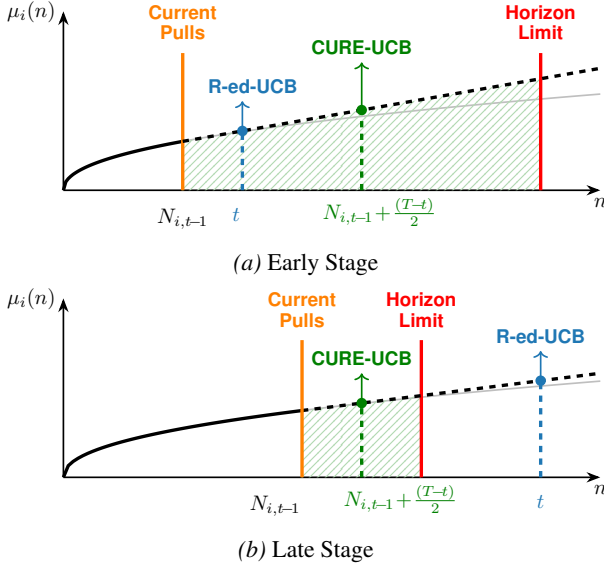


Figure 2. Comparison of estimation behaviors: horizon-aware (CURE-UCB) vs. horizon-agnostic (R-ed-UCB). The **Horizon Limit** denotes the maximum reachable point given the remaining trials. Since this horizon ($T - t$) is identical for all arms, we visualize CURE-UCB using its midpoint derived from the cumulative area; normalizing by this common factor preserves the arm ranking. (a) Early Stage: R-ed-UCB remains conservative due to small t , whereas CURE-UCB targets a point closer to the horizon limit, enabling aggressive exploration. (b) Late Stage: CURE-UCB shifts to exploitation within the limit, while R-ed-UCB overshoots into the impossible region.

4.2. Intuition: Comparison with Horizon-Agnostic Algorithms

To understand the mechanism of CURE-UCB, it is instructive to contrast its estimation objective with that of horizon-agnostic algorithms like R-ed-UCB (Metelli et al., 2022; Fiandri et al., 2024). While these methods capture the rising nature of rewards, they face inherent inefficiencies due to their inability to tailor strategies to the fixed horizon. An illustration of this comparison is given in Figure 2.

Instantaneous prediction While the ideal objective is to maximize the cumulative reward over the remaining horizon, estimating this aggregate value accurately is difficult without an explicit horizon T . Consequently, horizon-agnostic algorithms, such as R-ed-UCB, typically operate by estimating the expected reward at a specific future time step without prior knowledge of the total horizon. This design is effective for indefinite horizon settings, where identifying and committing to the arm with the highest growth rate is indeed the optimal long-term strategy.

Horizon adaptive prediction (CURE-UCB) In contrast, CURE-UCB dynamically adapts its strategy to the varying horizon. As established in Proposition 3.2, the optimal policy changes strictly based on the remaining horizon. Leveraging the known horizon T , CURE-UCB continuously recalibrates its valuation. By estimating the average reward

expected if the arm were played for the remaining horizon, the algorithm effectively aligns its decision-making with the optimal policy. This enables CURE-UCB to fluidly change its focus: when remaining horizon is sufficient, CURE-UCB invests arms with high potential, while prioritizing immediate returns when the remaining horizon is insufficient.

5. Analysis

In this section, we provide the theoretical analysis of the proposed CURE-UCB algorithm. Firstly, we demonstrate the superiority of our approach in deterministic “Linear-Then-Flat” (LTF) environments, proving that CURE-UCB strictly dominates representative horizon-agnostic strategies. Finally, we derive a general regret upper bound, guaranteeing the efficiency of our method across broad concave rising environments.

5.1. Superiority in Linear-Then-Flat (LTF) Setting

To substantiate the theoretical advantage of horizon awareness, we analyze the performance in a concrete structured environment. We focus on the “Linear-Then-Flat” (LTF) setting, which serves as a canonical example where the optimal strategy shifts sharply based on the horizon. In this setting, we demonstrate that CURE-UCB strictly outperforms R-ed-UCB (Metelli et al., 2022), a representative horizon-agnostic algorithm. We first formally define the deterministic ($\sigma=0$) LTF instance class:

Definition 5.1. (Linear-Then-Flat Instance) Let \mathfrak{U}_K denote the set of K -armed Linear-Then-Flat problem instances. For any instance $\mu \in \mathfrak{U}_K$, the expected reward of arm i at its n -th play is defined as:

$$\mu_i(n) = \min \{b_i, a_i \cdot n\} , \quad (7)$$

where $a_i > 0$ represents the growth rate (slope), $0 < b_i < 1$ represents maximum attainable reward. An arm i grows linearly with rate a_i until it reaches the capacity b_i , after which it yields a constant reward b_i .

Under this specific instance class, we establish the following theorem demonstrating the strict dominance of CURE-UCB over R-ed-UCB:

Theorem 5.2 (Strict Dominance in deterministic LTF). *Let π_{det}^{cure} denote the CURE-UCB algorithm with $h_i = 1$ and π_{det}^{red} denote the R-ed-UCB algorithm with $h_i = 1$. Consider a deterministic LTF problem instance $\mu \in \mathfrak{U}_K$ ($\sigma = 0$) and for any finite horizon T , the cumulative regret of CURE-UCB is always less than or equal to that of R-ed-UCB :*

$$Reg_{\mu}(\pi_{det}^{cure}, T) \leq Reg_{\mu}(\pi_{det}^{red}, T) . \quad (8)$$

The strict dominance result originates from the distinct capabilities in adhering to horizon-dependent optimality,

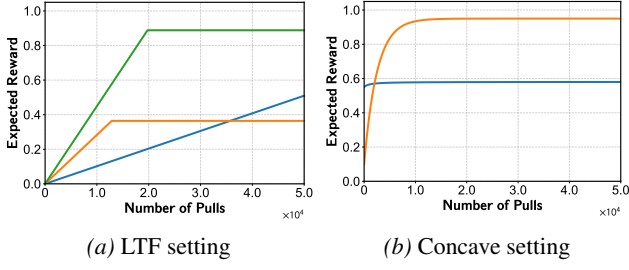


Figure 3. Example instances of synthesized environments. (a) The Linear-Then-Flat (LTF) setting, where the expected reward increases linearly before reaching a saturation point. (b) The concave setting, characterizing non-linear growth dynamics.

specifically when a high-growth arm becomes saturated. Initially, both algorithms prioritize arms with high growth rates. However, the difference occurs once the current high-growth arm reaches its capacity. At this point, the optimal strategy depends entirely on whether the remaining horizon is sufficient to justify switching to a new initially lower-reward arm. Leveraging the known horizon T , CURE-UCB precisely identifies this optimal switching moment. It calculates whether the accumulated future gain from the new arm exceeds the initial performance deficit within the remaining horizon. If the horizon is insufficient, CURE-UCB correctly identifies that sticking to the saturated arm aligns with the horizon-dependent optimality. In contrast, R-ed-UCB, lacking knowledge of T , finds it impossible to verify this condition. Driven by the estimated slope, it invariably switches to the new arm whenever it detects a high growth rate, failing to account for the fact that the remaining horizon is too short to recover the investment cost. This structural inability to determine the correct switching moment leads R-ed-UCB to incur wasteful exploration, resulting in strictly higher regret compared to CURE-UCB. The detailed proof is provided in Appendix B.

5.2. General Regret Upper Bound

To quantify the complexity of general RMAB instances beyond the LTF setting, we adapt the definition of *cumulative increment* from Metelli et al. (2022), which characterizes the total magnitude of reward growth.

Definition 5.3. (Cumulative increment) Let $\gamma_{\max}(n) := \max_{i \in [K]} \gamma_i(n)$ be the maximum instantaneous increment across all arms at the n -th play. For a horizon M and a parameter $q \in [0, 1]$, we define the *cumulative increment* $\Upsilon_\mu(M, q)$ as follows:

$$\Upsilon_\mu(M, q) := \sum_{n=1}^M (\gamma_{\max}(n))^q. \quad (9)$$

Leveraging this complexity measure, we establish the following regret upper bound, which guarantees the efficient

performance of CURE-UCB in general concave rising environments.

Theorem 5.4 (Regret upper bound for general case). *Let π_ϵ be CURE-UCB algorithm with $h_i = \lfloor \epsilon N_{i,t-1} \rfloor$. For $T > 0$, $q \in [0, 1]$, and $\epsilon \in (0, 0.5)$, we have the following regret upper bound:*

$$\begin{aligned} \text{Reg}_\mu(\pi_\epsilon, T) &\leq \frac{(1 + 2^{1+q})KT^q}{2} \Upsilon_\mu \left(\left\lceil (1 - 2\epsilon) \frac{T}{K} \right\rceil, q \right) \\ &+ \frac{3K}{\epsilon} (\sigma T)^{2/3} (\log T)^{1/3} (18 + 48\epsilon^2)^{1/3} + O(1) \end{aligned} \quad (10)$$

The derived upper bound establishes the theoretical soundness of the cumulative estimation approach. It confirms that CURE-UCB maintains the standard convergence rate characteristic of concave rising bandits. This result validates that explicitly targeting the cumulative reward is a safe and effective strategy, capable of handling the complexity of general environments while preserving the fundamental theoretical guarantees. The proof of Theorem 5.4 is provided in Appendix C.

6. Experiments

In this section, we evaluate CURE-UCB against state-of-the-art baselines in rising and non-stationary environments. We test two synthetic settings: (i) the Linear-Then-Flat (LTF) setting (Section 6.1) to confirm the strict dominance in Theorem 5.2, and (ii) the Concave setting (Section 6.2) to verify the regret bound presented in Theorem 5.4. We further demonstrate practical utility via online model selection (Section 6.3). Detailed specifications are in Appendix A.

Baselines We compare CURE-UCB against two categories of algorithms:

- **Rising bandit algorithms:** We adopt state-of-the art algorithms designed for the rising bandit framework, including R-ed-UCB (Metelli et al., 2022), ET-SWGTs (Fiandri et al., 2025), TI-UCB (Xia et al., 2024), and R-ed-AE (Amichay & Mansour, 2025).
- **Non-stationary bandit algorithms:** As the RMAB framework is an instance of non-stationary environments, we include representative algorithms handling dynamic rewards. These comprise sliding-window approaches (SW-UCB (Garivier & Moulines, 2011), SW-KL-UCB (Garivier & Cappé, 2011), SW-TS (Trovo et al., 2020)), as well as the restarting-based Rexp3 (Besbes et al., 2014) and the sequential elimination-based Ser4 (Allesiardo et al., 2017).

Detailed descriptions and pseudocode for all baseline algorithms are provided in Appendix E.

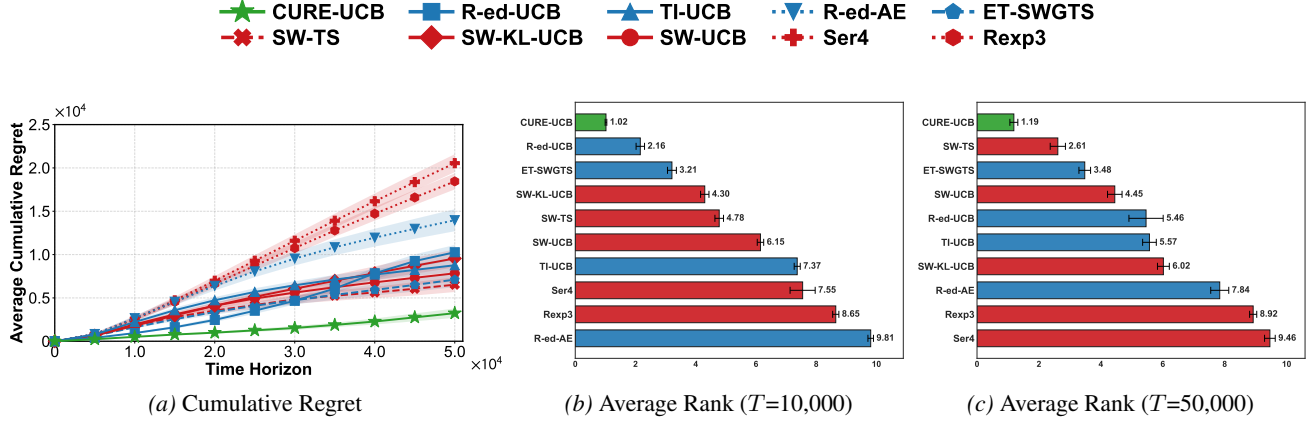


Figure 4. Performance Analysis in LTF Setting. (a) Cumulative regret as a function of the time horizon T . CURE-UCB consistently achieves the lowest regret across all horizons. (b, c) Average Rank at $T=10,000$ (short horizon) and $T=50,000$ (long horizon), respectively. Lower rank indicates better performance. CURE-UCB maintains the lowest rank in both horizons. Shaded regions and error bars denote 95% confidence intervals.

Evaluation Metrics We evaluate performance using Cumulative Regret, measuring the accumulated difference between the expected reward of the optimal policy and the algorithm. A key distinction in our analysis is the x-axis: since the optimal policy in the RMAB framework varies with the horizon T , and algorithms (including CURE-UCB) explicitly utilize T , we report the cumulative regret as a function of T , rather than intermediate time steps t . Additionally, to demonstrate robustness, we report the Average Rank of the algorithms, calculated over 100 independent problem instances at specific fixed horizons ($T=10,000$ and $50,000$).

6.1. Linear-Then-Flat Setting

To construct a rigorous evaluation environment for the Linear-Then-Flat (LTF) setting, we generated problem instances strictly following the formulation in Definition 5.1, as visually depicted in Figure 3a. Within this framework, we enforced structural diversity by randomizing the parameters for each arm, rather than relying on fixed configurations (detailed specifications in Appendix A). This randomized generation leads to mixed scenarios: some instances have optimal arms with high initial rewards (favoring reactive non-stationary algorithms), while others have steep growth rates (favoring rising bandit algorithms).

The structural diversity described above leads to fluctuating rankings among the baselines, as they are specialized for specific dynamics (as depicted in Figure 4b and c). In contrast, CURE-UCB demonstrates remarkable stability, consistently achieving superior rankings regardless of these variations. Furthermore, Figure 4a confirms that CURE-UCB yields the lowest cumulative regret. This demonstrates that CURE-UCB successfully adapts to the underlying structure by identifying whether immediate exploitation or long-

term investment is required, effectively outperforming all baselines in both stability and performance.

6.2. Concave Setting

Following the analysis in the strictly structured LTF setting, we extend our evaluation to the concave setting to demonstrate generalization under relaxed assumptions. Unlike the LTF model, we constructed this environment using arbitrary concave functions to simulate diverse non-linear dynamics (detailed specifications in Appendix A). Within this broader framework, we orchestrate a structural conflict between the early peaker and the late bloomer, where the optimal arm is strictly determined by the horizon length T .

As shown in Figure 5a, CURE-UCB consistently records the lowest average cumulative regret across all horizons. Notably, R-ed-AE also demonstrates robust performance in this setting. This is driven by its horizon-awareness, which allows it to navigate the conflict between immediate rewards and future growth effectively. Consequently, its regret growth becomes nearly negligible towards the end of the horizon. We attribute this to its elimination-based nature, which naturally ceases exploration on discarded arms, and its resilience to the gradual curvature of concave functions.

For other baselines, we observe a distinct performance shift specifically in the long horizon. As shown in Figure 5c ($T=50,000$), rising bandit algorithms (blue) clearly decouple from and outperform non-stationary algorithms (red). This separation occurs because non-stationary methods do not account for the rising property of the reward functions. Consequently, they fail to identify the late bloomer arm and instead adhere to the early peaker. In contrast, rising bandit algorithms are structurally capable of capturing this growth potential.

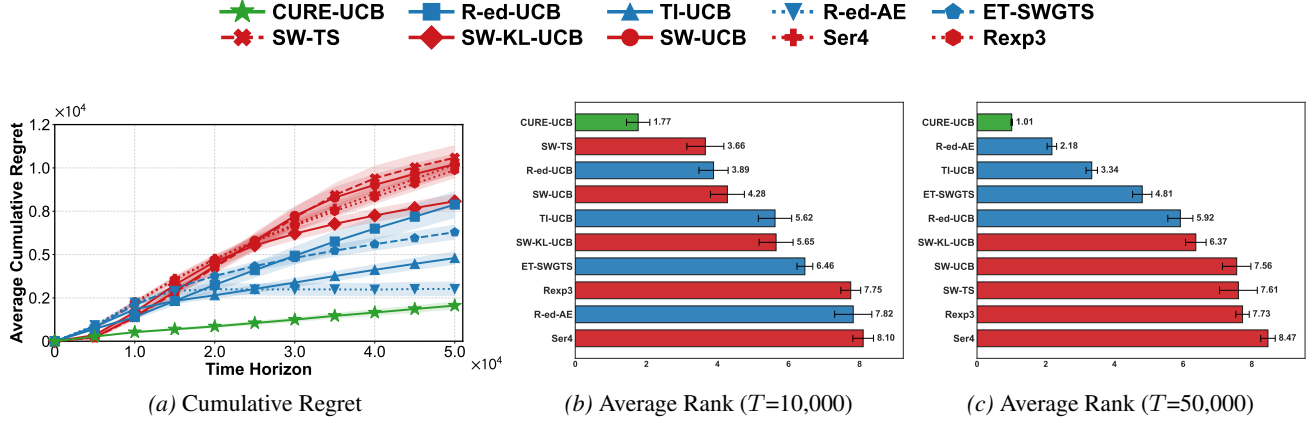


Figure 5. Performance Analysis in Concave Setting. (a) Cumulative regret as a function of the time horizon T . CURE-UCB consistently achieves the lowest regret across all horizons. (b, c) Average Rank at $T=10,000$ (short horizon) and $T=50,000$ (long horizon), respectively. Lower rank indicates better performance. CURE-UCB maintains the lowest rank in both horizons. Shaded regions and error bars denote 95% confidence intervals.

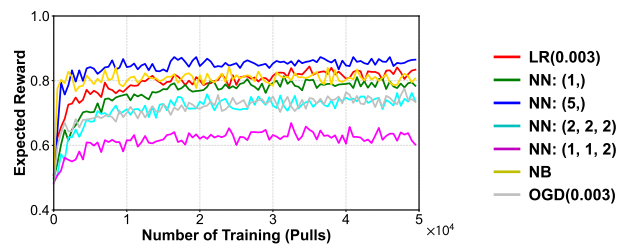


Figure 6. Reward Dynamics in Online Model Selection (IMDB). Each line represents the validation accuracy of a distinct learning model configuration over time ($T=50,000$). Unlike synthetic settings, these real-world learning curves exhibit significant volatility and do not strictly adhere to smooth concave growth, presenting a challenging environment for horizon-dependent optimization.

6.3. Online Model Selection (IMDB)

To demonstrate the practical applicability of our framework, we investigate the problem of online model selection for text generation tasks using the IMDB dataset (Maas et al., 2011). In this task, each arm represents a distinct learning model (e.g., neural networks with different hyperparameters) being trained on the sentiment analysis task. The objective is to identify the model that yields the highest cumulative validation accuracy within a finite training budget T , which serves as the fixed horizon.

As illustrated in Figure 6, real-world training curves exhibit persistent fluctuations and noise, presenting a significantly more challenging environment compared to synthetic settings. Despite this high variance, CURE-UCB achieves competitive performance comparable to the strongest baseline, R-ed-UCB, as shown in Figure 7. Notably, at $T = 50,000$, the average regret of CURE-UCB aligns with the lower confidence bound of R-ed-UCB, indicating stable performance even in noise-dominated regimes.

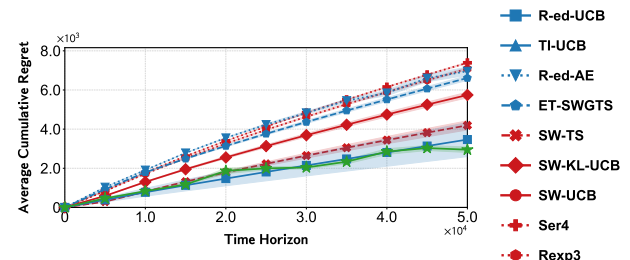


Figure 7. Cumulative Regret on IMDB Dataset. Performance comparison of CURE-UCB against baselines over a horizon of $T=50,000$, based on the reward functions depicted in Figure 6. Shaded regions denote 95% confidence intervals.

7. Conclusion

In this paper, we addressed the structural challenge of horizon-dependent optimality in Rising Multi-Armed Bandits, where the optimal strategy is strictly dictated by the finite time horizon. We highlighted that horizon-agnostic algorithms suffer from an unavoidable inefficiency, leading to suboptimal performance. To overcome this limitation, we proposed CURE-UCB, a horizon-aware algorithm that explicitly estimates the aggregate future potential of each arm. Our theoretical analysis established a regret upper bound for general concave rising bandits and proved the strict dominance of our method in Linear-Then-Flat (LTF) settings, demonstrating its capability to prevent wasteful exploration of saturated arms. Furthermore, extensive empirical evaluations in LTF and Concave settings, along with practical online model selection tasks, confirmed that CURE-UCB consistently achieves competitive or superior performance compared to state-of-the-art baselines. These results underscore the necessity of horizon awareness in finite-horizon rising bandits. Future work may investigate the extension of this framework to complex real-world applications such as LLM fine-tuning or robotics.

Impact Statements

This paper presents work whose goal is to advance the field of machine learning. There are many potential societal consequences of our work, none of which we feel must be specifically highlighted here.

References

Allesiardo, R., Féraud, R., and Maillard, O.-A. The non-stationary stochastic multi-armed bandit problem. *International Journal of Data Science and Analytics*, 3(4): 267–283, 2017.

Amichay, O. and Mansour, Y. Rising rested mab with linear drift. *arXiv preprint arXiv:2501.04403*, 2025.

Arora, R., Dekel, O., and Tewari, A. Online bandit learning against an adaptive adversary: from regret to policy regret. *arXiv preprint arXiv:1206.6400*, 2012.

Besbes, O., Gur, Y., and Zeevi, A. Stochastic multi-armed-bandit problem with non-stationary rewards. *Advances in neural information processing systems*, 27, 2014.

Fiandri, M., Metelli, A. M., and Trovo, F. Rising rested bandits: Lower bounds and efficient algorithms. *arXiv preprint arXiv:2411.14446*, 2024.

Fiandri, M., Metelli, A. M., and Trovò, F. Thompson sampling-like algorithms for stochastic rising bandits. *arXiv preprint arXiv:2505.12092*, 2025.

Garivier, A. and Cappé, O. The kl-ucb algorithm for bounded stochastic bandits and beyond. In *Proceedings of the 24th annual conference on learning theory*, pp. 359–376. JMLR Workshop and Conference Proceedings, 2011.

Garivier, A. and Moulines, E. On upper-confidence bound policies for switching bandit problems. In *International conference on algorithmic learning theory*, pp. 174–188. Springer, 2011.

Heidari, H., Kearns, M. J., and Roth, A. Tight policy regret bounds for improving and decaying bandits. In *IJCAI*, pp. 1562–1570, 2016.

Li, L., Jamieson, K., DeSalvo, G., Rostamizadeh, A., and Talwalkar, A. Hyperband: A novel bandit-based approach to hyperparameter optimization. *Journal of Machine Learning Research*, 18(185):1–52, 2018.

Li, Y., Jiang, J., Gao, J., Shao, Y., Zhang, C., and Cui, B. Efficient automatic cash via rising bandits. *Proceedings of the AAAI Conference on Artificial Intelligence*, 34: 4763–4771, 2020.

Maas, A., Daly, R. E., Pham, P. T., Huang, D., Ng, A. Y., and Potts, C. Learning word vectors for sentiment analysis. In *Proceedings of the 49th annual meeting of the association for computational linguistics: Human language technologies*, pp. 142–150, 2011.

Metelli, A. M., Trovo, F., Pirola, M., and Restelli, M. Stochastic rising bandits. In *International Conference on Machine Learning*, pp. 15421–15457. PMLR, 2022.

Song, S., Yoon, Y., Wang, S., Chen, W., and Ok, J. Combinatorial rising bandit. *arXiv preprint arXiv:2412.00798*, 2024.

Trovò, F., Paladino, S., Restelli, M., and Gatti, N. Sliding-window thompson sampling for non-stationary settings. *Journal of Artificial Intelligence Research*, 68:311–364, 2020.

Xia, Y., Kong, F., Yu, T., Guo, L., Rossi, R. A., Kim, S., and Li, S. Which lilm to play? convergence-aware online model selection with time-increasing bandits. In *Proceedings of the ACM on Web Conference 2024*, pp. 4059–4070, 2024.

Yoon, Y., Lee, G., Ahn, S., and Ok, J. Breadth-first exploration on adaptive grid for reinforcement learning. In *Forty-first International Conference on Machine Learning*, 2024.

This material provides proof of theorems, details of environments and baselines, and additional experimental results:

- **Appendix A:** Detailed explanation for experiment
- **Appendix B:** Proof of Theorem 5.2
- **Appendix C:** Proof of Theorem 5.4
- **Appendix D:** Proof of Lemmas
- **Appendix E:** Detailed description and hyperparameter setting of the baselines in Section 6.

A. Detailed explanation for experiment

A.1. Synthetic Environment Generation

In this section, we explain how we randomly generate the problem instances.

A.1.1. LINEAR-THEN-FLAT (LTF) SETTING

We generated 100 independent problem instances for the LTF setting. Each instance consists of $K \in \{2, 3, 4, 5\}$ arms, where each arm's reward function follows the form $\mu_i(n) = \min(b_i, a_i \cdot n)$. The saturation level b_i is sampled uniformly from $[0.1, 1.0]$, and the saturation time t_{sat} is randomly selected from $[0.05T, T]$ for $T = 50,000$. The slope is then determined as $a = b/t_{\text{sat}}$.

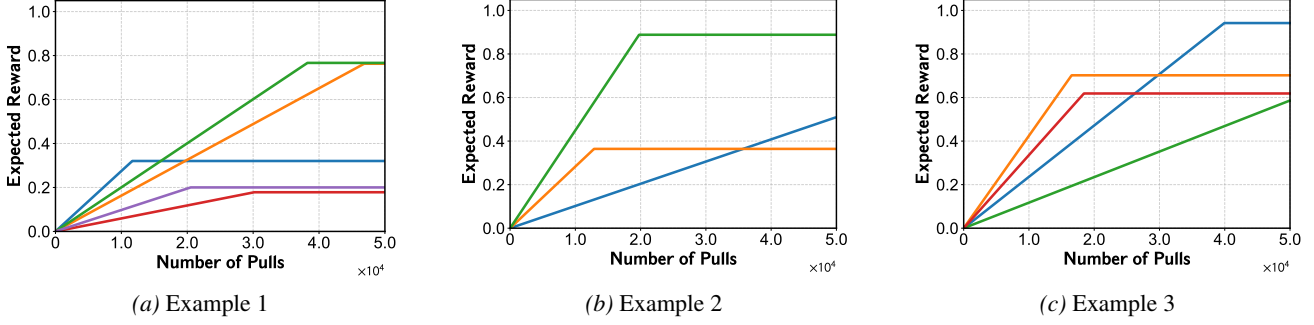


Figure 8. Example instances of LTF Setting.

A.1.2. CONCAVE SETTING

We generate 100 independent problem instances for the Concave setting. Each instance consists of $K \in \{2, 3, 4, 5\}$ arms. In each instance, we explicitly include two structured arms: early peaker and late bloomer. The late bloomer (optimal arm) is constrained to have low early rewards but high late rewards: $\mu(0) \approx 0.1$ and $\mu(T) \approx 0.95$. The early peaker (deceptive arm) is constrained to have better early while being worse asymptotically: $\mu(0) \approx 0.55$ and $\mu(T) \approx 0.58$. For remaining arms, the reward of each arm follows a bounded, saturating curve of the form

$$\mu(t) = s + (L - s) g(t) ,$$

where s is sampled uniformly from $[0.05, 0.35]$ and L is sampled uniformly from $[0.90, 0.99]$, and For $g(t)$, we use one of the following normalized saturating growth functions $g(t) \in [0, 1]$: The shape parameters are chosen such that all arms reach at least 75% of their final value by $t = 10000$.

$$g_{\text{rat}}(t; k) = \frac{\frac{t}{T+k}}{\frac{T}{T+k}}, \quad g_{\text{exp}}(t; k) = \frac{1 - e^{-kt}}{1 - e^{-kT}}, \quad g_{\text{atan}}(t; k) = \frac{\arctan(kt)}{\arctan(kT)}.$$

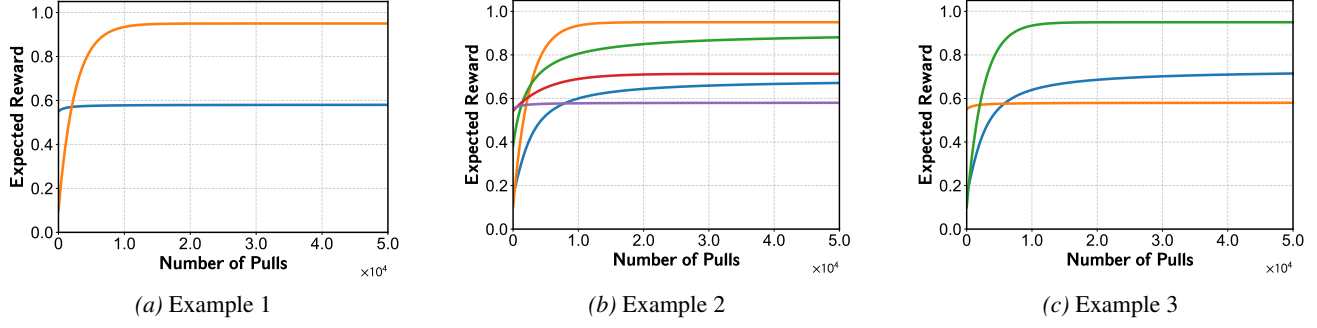


Figure 9. Example instances of Concave Setting.

B. Proof of Theorem 5.2

In this section, we provide the proof for Theorem 5.2. Since we consider deterministic reward setting (e.g., $\sigma=0$), CURE-UCB and R-ed-UCB (Metelli et al., 2022) can be simplified because the policy always receive exactly expected reward. We do not need to consider large sliding-window and can just set $h_i = 1$. For the reader's convenience, we provide pseudocode for the algorithm employed in this proof.

Algorithm 2 R-ed-UCB (Deterministic Version)

```

1: Input: Number of arms  $K$ ,
2: Initialize: For each arm  $i \in [K]$ , set  $N_i \leftarrow 0$ .
3: for  $t = 1, \dots, T$  do
4:   if  $t \leq K$  then
5:     Play arm  $I_t = (t \bmod K) + 1$ .
6:   else
7:     Compute deterministic index  $B_i(t)$  for each arm  $i \in [K]$  based on equation 11.
8:     Select arm  $I_t = \arg \max_{i \in [K]} B_i(t)$ .
9:   end if
10:  Update counter  $N_{I_t} \leftarrow N_{I_t} + 1$ .
11:  Update state using the deterministic mean reward  $\mu_{I_t, t}$ .
12: end for

```

Algorithm 3 CURE-UCB (Deterministic Version)

```

1: Input: Horizon  $T$ , Number of arms  $K$ 
2: Initialize: For each arm  $i \in [K]$ , set  $N_i \leftarrow 0$ .
3: for  $t = 1, \dots, T$  do
4:   if  $t \leq K$  then
5:     Play arm  $I_t = (t \bmod K) + 1$ .
6:   else
7:     Compute deterministic index  $B_i(t)$  for each arm  $i \in [K]$  based on equation 12.
8:     Select arm  $I_t = \arg \max_{i \in [K]} B_i(t)$ .
9:   end if
10:  Update counter  $N_{I_t} \leftarrow N_{I_t} + 1$ .
11:  Update state using the deterministic mean reward  $\mu_{I_t, t}$ .
12: end for

```

Firstly, we recall index of R-ed-UCB in deterministic setting, which is given in Section 4.2 of (Metelli et al., 2022)

$$B_i^{red}(t) := \mu_i(N_{i,t-1}) + (t - N_{i,t-1})\gamma_i(N_{i,t-1} - 1). \quad (11)$$

The index of CURE-UCB in deterministic setting is given as follows:

$$B_i^{cure}(t) := \mu_i(N_{i,t-1}) + \frac{(T-t)}{2} \gamma_i(N_{i,t-1} - 1). \quad (12)$$

In LTF setting, the expected reward of every arm $i \in [K]$ is given as follows:

$$\mu_i(n) = \min(b_i, a_i n). \quad (13)$$

For every arm, we define $c_i := \frac{b_i}{a_i}$, which means the time steps required to make arm i saturated. For convenience, we fix some T and assume that the arms are ordered in descending order with respect to a_i . That is, $a_1 > a_2 > \dots > a_K$. Let $I_{cure}(T)$ and $I_{red}(T)$ denote the set of arms that are played at least once until time T by CURE-UCB and by R-ed-UCB respectively. Then, we assert the following claim:

Claim 1. Both $I_{cure}(T)$ and $I_{red}(T)$ grows monotonically with T , and its element appear in ascending order $\{1, 2, \dots, K\}$.

This claim trivially holds because we assume that all arms increase linearly starting from zero. Consequently, both algorithms are compelled to select the arms in the order of decreasing order with respect to a_i .

Then, we now characterize the behavior of the two algorithms. Firstly, we consider CURE-UCB:

Claim 2. Let i_{cure}^* be defined as follows:

$$i_{cure}^* := \arg \max_{i \in I_{cure}(T)} b_i. \quad (14)$$

Then, CURE-UCB selects each arm $i \in I_{cure}(T) \setminus i_{cure}^*$ exactly c_i times, and select arm i_{cure}^* for the remaining $T - \sum_{i \in I_{cure} \setminus i_{cure}^*} c_i$ times.

We begin by an observation that if CURE-UCB selects some arm i for the first time at time t_i , then it must continue to select arm i for the next $c_i - 1$ rounds. The fact that CURE-UCB selects arm i at time t_i implies that the index of arm i , $B_i^{cure}(t_i)$, is the largest among all arms. Then, at time $t_i + 1$, we observe that $B_i^{cure}(t_i + 1) \geq B_i^{cure}(t_i)$, while for any other arm $j \in [K]$, we have $B_j^{cure}(t_i + 1) \leq B_j^{cure}(t_i)$. Therefore, CURE-UCB also selects arm i at time $t_i + 1$. This continues until arm i becomes flat, namely for c_i rounds.

Also, we observe that if some arm i , after being selected c_i times, is selected again at some time t'_i , then arm i will continue to be selected for the remaining time. We consider two cases for another arm j : either by time t'_i it has already been selected c_j times, or it has not. If arm j has already been selected c_j times, then the fact that arm i is selected at time t'_i implies that $b_i > b_j$. It is then immediate that, for the remaining time, the index of arm i remains greater than that of arm j . If arm j has been selected fewer than c_j times, then by the previous observation, arm j has not been selected at all yet. At time $t'_i + 1$, comparing the indices yields

$$B_i^{cure}(t'_i + 1) = B_i^{cure}(t'_i) \quad (15)$$

for arm i , and

$$B_j^{cure}(t'_i + 1) = B_j^{cure}(t'_i) - \frac{a_j}{2} \quad (16)$$

for arm j . For arm j to be selected instead of arm i at time $t'_i + 1$, it would be necessary that $\frac{a_j}{2} < b_i$. Then, since $B_j^{cure}(t'_i + 1) \leq B_j^{cure}(t'_i) \leq B_i^{cure}(t'_i) \leq B_i^{cure}(t'_i + 1)$, which means that arm i will be selected at time $t'_i + 1$. The same reasoning can be applied repeatedly for every round from $t = t'_i + 1$ up to $T - 1$.

Based on the two preceding observations, we prove the claim. First, if every arm in $I_{cure}(T)$ has been selected at least c_i times, then by preceding observations, our claim is immediate. Now, suppose that there exists an arm in $I_{cure}(T)$ that has been selected at most c_i times. By the first observation, such an arm must be unique. Let us denote this unique arm by i' . Let t' denote the time at which arm i' is firstly selected. Then, by the first observation, we have $(T - t') < c_{i'}$. Define b' as the maximum value of b_i among the arms in $i \in I_{cure}(T) \setminus i'$. Then, at time t' , we have

$$\frac{a_{i'}}{2}(T - t')^2 > b'(T - t'). \quad (17)$$

Rearranging this inequality gives

$$(T - t') > \frac{2b'}{a_{i'}}. \quad (18)$$

Combining this with the earlier result $(T - t') < c_{i'}$, we obtain $b_{i'} > 2b'$. Hence, i' corresponds to i_{cure}^* , and the proof of the claim is complete.

Now, we make a claim for R-ed-UCB:

Claim 3. Let i'_{red} be defined as follows:

$$i'_{\text{red}} := \arg \min_{i \in I_{\text{red}}(T)} a_i. \quad (19)$$

Then, R-ed-UCB selects each arm $i \in I_{\text{red}}(T) \setminus \{i'_{\text{red}}\}$ at least c_i times.

Similarly, We begin by an observation that if CURE-UCB selects some arm i for the first time at time t_i , then it must continue to select arm i for the next $c_i - 1$ rounds. By the design of R-ed-UCB, at time t_i , among the arms that are not selected, arm i is the one with the largest slope. Moreover, all arms with larger slopes than arm i must already have been pulled at least c_i times. Otherwise, at time c_i , R-ed-UCB would select another arm instead of arm i . Therefore, it is clear that arm i will be selected from time t_i to $t_i + c_i$. However, unlike CURE-UCB, note that R-ed-UCB cannot guarantee that these arms are pulled exactly c_i times.

Then, we make following claim for relationship between $I_{\text{cure}}(T)$ and $I_{\text{red}}(T)$.

Claim 4.

$$I_{\text{cure}}(T) \subseteq I_{\text{red}}(T) \quad (20)$$

Let T_i^{red} be the first total time when i is included in $I_{\text{red}}(T_i^{\text{red}})$. Then, we can write T_i^{red} as follows:

$$T_1^{\text{red}} = 1 \quad (21)$$

$$T_2^{\text{red}} = \frac{b_1}{a_2} \quad (22)$$

$$T_3^{\text{red}} = \max \left\{ T_2^{\text{red}} + c_2, \frac{\max(b_1, b_2)}{a_3} \right\} \quad (23)$$

$$\dots \quad (24)$$

$$T_k^{\text{red}} = \max \left\{ T_{k-1}^{\text{red}} + c_{k-1}, \frac{\max(b_1, b_2, \dots, b_{k-1})}{a_k} \right\} \quad (25)$$

Similarly, let T_i^{cure} be the first total time when i is included in $I_{\text{cure}}(T_i^{\text{cure}})$. Then, we can write T_i^{cure} as follows:

$$T_1^{\text{cure}} = 1 \quad (26)$$

$$T_2^{\text{cure}} = c_1 + \frac{2b_1}{a_2} \quad (27)$$

$$T_3^{\text{cure}} = c_1 + c_2 + \frac{2 \max(b_1, b_2)}{a_3} \quad (28)$$

$$\dots \quad (29)$$

$$T_k^{\text{cure}} = \sum_{i=1}^{k-1} c_i + \frac{2 \max(b_1, b_2, \dots, b_{k-1})}{a_k} \quad (30)$$

Then, it suffices to show that $T_i^{\text{red}} \leq T_i^{\text{cure}}$ for proof. To show it, we utilize induction. For base case ($i = 2$), it is clear that $T_2^{\text{red}} \leq T_2^{\text{cure}}$. Then, assuming that $T_{k-1}^{\text{red}} \leq T_{k-1}^{\text{cure}}$, we can easily show that $T_k^{\text{red}} \leq T_k^{\text{cure}}$, which completes proof. Then, we proceed the proof. Let $S^{\text{cure}}(T)$ be the set of arms in $I_{\text{cure}}(T)$ that have been played c_i times. Then, by Claim 4, all arms in $S^{\text{cure}}(T)$ are guaranteed to have been played at least c_i times by R-ed-UCB as well. Then, we can assume that all arms in $S^{\text{cure}}(T)$ have already been played c_i times, and consider a new regret minimization problem for remaining time $T - \sum_{i \in S^{\text{cure}}(T)} c_i$. Then, we can see that in this problem the optimal policy is to keep selecting a single arm, and CURE-UCB behaves exactly the same as the optimal policy. Therefore, it is guaranteed that CURE-UCB has better regret than R-ed-UCB.

C. Proof of Theorem 5.4

Proof. For well-estimated event, we define $\hat{\mu}_i(t)$ and $\tilde{\mu}_i(t)$ as follows:

$$\bar{\mu}_i(t) := \frac{1}{h_i} \sum_{l=N_{i,t-1}-h_i+1}^{N_{i,t-1}} \left(X_i(l) + \frac{(T-t)}{2} \frac{X_i(l) - X_i(l-h_i)}{h_i} \right) \quad (31)$$

$$\tilde{\mu}_i(t) := \frac{1}{h_i} \sum_{l=N_{i,t-1}-h_i+1}^{N_{i,t-1}} \left(\mu_i(l) + \frac{(T-t)}{2} \frac{\mu_i(l) - \mu_i(l-h_i)}{h_i} \right) \quad (32)$$

$$\beta_i(t) := \sigma \sqrt{\frac{2[3(T-t)^2 + 8h_i^2] \log t^3}{4h_i^3}} \quad (33)$$

$$\hat{\mu}_i(t) := \tilde{\mu}_i(t) + \beta_i(t) . \quad (34)$$

We define well-estimated event \mathcal{E}_t as follows:

$$\mathcal{E}_{i,t} := \{|\tilde{\mu}_i(t) - \hat{\mu}_i(t)| \leq \beta_i(t)\} , \quad (35)$$

$$\mathcal{E}_t := \cap_{i \in [K]} \mathcal{E}_{i,t} . \quad (36)$$

Then, we rewrite the regret as follows:

$$Reg_{\mu}(\pi, T) = \sum_{t=1}^T \mathbb{E} [\mu_{i^*}(t) - \mu_{i_t}(N_{i_t,t})] \quad (37)$$

$$= \sum_{t=1}^T \mathbb{E} [(\mu_{i^*}(t) - \mu_{i_t}(N_{i_t,t})) \mathbb{1}\{\mathcal{E}_t\}] + \sum_{t=1}^T \mathbb{E} [(\mu_{i^*}(t) - \mu_{i_t}(N_{i_t,t})) \mathbb{1}\{\mathcal{E}_t^c\}] \quad (38)$$

$$\leq \underbrace{\sum_{t=1}^T \mathbb{E} [(\mu_{i^*}(t) - \mu_{i_t}(N_{i_t,t})) \mathbb{1}\{\mathcal{E}_t\}]}_{(A)} + \underbrace{\sum_{t=1}^T \mathbb{E} [\mathbb{1}\{\mathcal{E}_t^c\}]}_{(B)} . \quad (39)$$

Then, we bound (B) term.

$$(B) = \sum_{t=1}^T \mathbb{P}(\mathcal{E}_t^c) \quad (40)$$

$$= 1 + \sum_{t=2}^T \mathbb{P} \left(\bigcup_{i \in [K]} \mathcal{E}_{i,t}^c \right) \quad (41)$$

$$\leq 1 + \sum_{t=2}^T \sum_{i \in [K]} \mathbb{P}(\mathcal{E}_{i,t}^c) , \quad (42)$$

where equation 41 holds due to De Morgan's Law and equation 42 follows from the application of the union bound. From Lemma D.1, we have:

$$\sum_{t=2}^T \sum_{i \in [K]} \mathbb{P}(\mathcal{E}_{i,t}^c) \leq \sum_{t=2}^T \sum_{i \in [K]} 2t^{-2} \leq \frac{K\pi^2}{3} . \quad (43)$$

Now, we bound (A) term. Under \mathcal{E} , we can decompose (A) term as follows:

$$\mu_{i^*}(t) - \mu_{i_t}(N_{i_t,t}) \leq \mu_{i^*}(t) - \mu_{i_t}(N_{i_t,t}) + B_{i_t}(t) - B_{i^*}(t) \quad (44)$$

$$= \mu_{i^*}(t) - \mu_{i_t}(N_{i_t,t}) + (\bar{\mu}_{i_t}(t) + \beta_{i_t}(t)) - (\bar{\mu}_{i^*}(t) + \beta_{i^*}(t)) \quad (45)$$

$$\leq \mu_{i^*}(t) - \mu_{i_t}(N_{i_t,t}) + (\tilde{\mu}_{i_t}(t) + 2\beta_{i_t}(t)) - \tilde{\mu}_{i^*}(t) \quad (46)$$

$$= \underbrace{\mu_{i^*}(t) - \tilde{\mu}_{i^*}(t)}_{(A1)} + \underbrace{\tilde{\mu}_{i_t}(t) - \mu_{i_t}(N_{i_t,t})}_{(A2)} + \underbrace{2B_{i_t}(t)}_{(A3)}, \quad (47)$$

where equation 46 holds by the definition of \mathcal{E} . Then, we bound (A1) term. We can rewrite (A1) term as follows:

$$(A1) = \mu_{i^*}(t) - \frac{1}{h_{i^*}} \sum_{l=N_{i^*,t-1}-h_{i^*}+1}^{N_{i^*,t-1}} \left(\mu_i(l) + \frac{(T-t)}{2} \frac{\mu_{i^*}(l) - \mu_{i^*}(l-h_{i^*})}{h_{i^*}} \right) \quad (48)$$

$$= \frac{1}{h_{i^*}} \sum_{l=N_{i^*,t-1}-h_{i^*}+1}^{N_{i^*,t-1}} \left(\mu_{i^*}(t) - \mu_{i^*}(l) - \frac{(T-t)}{2} \frac{\mu_{i^*}(l) - \mu_{i^*}(l-h_{i^*})}{h_{i^*}} \right) \quad (49)$$

$$= \frac{1}{h_{i^*}} \sum_{l=N_{i^*,t-1}-h_{i^*}+1}^{N_{i^*,t-1}} \left(\mu_{i^*}(t) - \mu_{i^*}(l) - \frac{(T-t)}{2h_{i^*}} \sum_{k=l-h_{i^*}}^{l-1} \gamma_{i^*}(k) \right) \quad (50)$$

$$\leq \frac{1}{h_{i^*}} \sum_{l=N_{i^*,t-1}-h_{i^*}+1}^{N_{i^*,t-1}} \left(\mu_{i^*}(t) - \mu_{i^*}(l) - \frac{(T-t)}{2} \gamma_{i^*}(l-1) \right) \quad (51)$$

$$\leq \frac{1}{h_{i^*}} \sum_{l=N_{i^*,t-1}-h_{i^*}+1}^{N_{i^*,t-1}} \left(\max \left\{ 0, \frac{3t-2l-T}{2} \gamma_{i^*} \left(\frac{T-t}{2} \right) \right\} \right) \quad (52)$$

$$\leq \frac{1}{h_{i^*}} \sum_{l=N_{i^*,t-1}-h_{i^*}+1}^{N_{i^*,t-1}} T \gamma_{i^*} \left(\frac{T-t}{2} \right) \quad (53)$$

$$= T \gamma_{i^*} \left(\frac{T-t}{2} \right), \quad (54)$$

where equation 50 holds by the definition of γ_i and equation 51 holds by concavity assumption, (i.e., $\gamma_i(n)$ is decreasing over n) and equation 52 holds by Lemma D.2.

With summation, we have:

$$\sum_{t=1}^T (A1) \leq \sum_{t=1}^T T \gamma_{i^*} \left(\frac{T-t}{2} \right) \quad (55)$$

$$\leq \sum_{t=1}^T T \gamma_{i^*} \left(\left\lceil \frac{T-t}{2} \right\rceil \right) \quad (56)$$

$$\leq \sum_{t=1}^{T/2} 2T \gamma_{i^*}(t) \quad (57)$$

$$\leq 2T \sum_{t=1}^T \gamma_{\max}(t), \quad (58)$$

where equation 57 holds by definition of floor function. Then, we utilize the assumption that $(A1) \in [0, 1]$

$$\sum_{t=1}^T (A1) \leq \sum_{t=1}^T \min(1, A1) \quad (59)$$

$$\leq 2K + \sum_{t=2K+1}^T \min \{1, 2T \gamma_{\max}(t)\} \quad (60)$$

$$\leq 2K + 2^q T^q \sum_{t=2K+1}^T \gamma_{\max}(t)^q \quad (61)$$

$$\leq 2K + 2^q K T^q \Upsilon_{\mu} \left(\left\lceil \frac{T}{K} \right\rceil, q \right), \quad (62)$$

where equation 61 holds since when $\min \{1, x\} \leq \min \{1, x\}^q \leq x^q$ for any $x \geq 0$ and equation 62 holds by Lemma C.2. from (Metelli et al., 2022).

Then, we bound (A2) term.

$$(A2) = \frac{1}{h_{i_t}} \sum_{l=N_{i_t,t-1}-h_{i_t}+1}^{N_{i_t,t-1}} \left(\mu_{i_t}(l) + \frac{(T-t)}{2} \frac{\mu_{i_t}(l) - \mu_{i_t}(l-h_{i_t})}{h_{i_t}} \right) - \mu_{i_t}(N_{i_t,t}) \quad (63)$$

$$= \frac{1}{h_{i_t}} \sum_{l=N_{i_t,t-1}-h_{i_t}+1}^{N_{i_t,t-1}} \left(\mu_{i_t}(l) + \frac{(T-t)}{2} \frac{\mu_{i_t}(l) - \mu_{i_t}(l-h_{i_t})}{h_{i_t}} - \mu_{i_t}(N_{i_t,t}) \right) \quad (64)$$

$$\leq \frac{1}{h_{i_t}} \sum_{l=N_{i_t,t-1}-h_{i_t}+1}^{N_{i_t,t-1}} \frac{(T-t)}{2} \frac{\mu_{i_t}(l) - \mu_{i_t}(l-h_{i_t})}{h_{i_t}} \quad (65)$$

$$= \frac{(T-t)}{2h_{i_t}} \sum_{l=N_{i_t,t-1}-h_{i_t}+1}^{N_{i_t,t-1}} \sum_{k=l-h_{i_t}}^{l-1} \frac{1}{h_{i_t}} \gamma_{i_t}(k) \quad (66)$$

$$\leq \frac{(T-t)}{2h_{i_t}} \sum_{l=N_{i_t,t-1}-h_{i_t}+1}^{N_{i_t,t-1}} \gamma_{i_t}(l-h_{i_t}) \quad (67)$$

$$\leq \frac{(T-t)}{2} \gamma_{i_t}(N_{i_t,t-1} - 2h_{i_t} + 1), \quad (68)$$

where equation 65 holds since $\mu_i(n)$ is non-decreasing and $l \leq N_{i_t,t-1} \leq N_{i_t,t}$ and equation 67 holds by concavity assumption.

As before, we can utilize the assumption that $(A2) \leq [0, 1]$:

$$\sum_{t=1}^T (A2) \leq \sum_{t=1}^T \min \left\{ 1, \sum_{t=1}^T \frac{T-t}{2} \gamma_{i_t}(N_{i_t,t-1} - 2h_{i_t} + 1) \right\} \quad (69)$$

$$\leq 2K + \sum_{t=2K+1}^T \min \left\{ 1, \frac{T}{2} \gamma_{i_t}(N_{i_t,t-1} - 2h_{i_t} + 1) \right\} \quad (70)$$

$$\leq 2K + \sum_{t=2K+1}^T \min \left\{ 1, \frac{T}{2} \gamma_{i_t}((1-2\epsilon)N_{i_t,t-1}) \right\} \quad (71)$$

$$\leq 2K + \frac{KT^q}{2} \Upsilon_{\mu} \left(\left\lceil \frac{(1-2\epsilon)T}{K} \right\rceil, q \right), \quad (72)$$

where equation 72 holds by Lemma C.2. from (Metelli et al., 2022).

Then, we bound (A3) term. We also utilize the fact that the regret for one time step cannot precede 1.

$$\begin{aligned} \sum_{t=1}^T (A3) &\leq \sum_{i=1}^K \sum_{j=1}^{N_{i,T}} \min \left\{ 1, 2\sigma \sqrt{\frac{2[3T^2 + 8(\epsilon j)^2]3 \log T}{4(\epsilon j)^3}} \right\} \\ &\leq K \left\lceil \frac{1}{\epsilon} \right\rceil \sum_{i=1}^K \sum_{j=\lceil \frac{1}{\epsilon} \rceil + 1}^{N_{i,T}} \min \left\{ 1, 2\sigma \sqrt{\frac{2[3T^2 + 8(\epsilon j)^2]3 \log T}{4(\epsilon j)^3}} \right\} \end{aligned}$$

$$\begin{aligned}
 &\leq K \left\lceil \frac{1}{\epsilon} \right\rceil + \sum_{i=1}^K \sum_{j=\lceil \frac{1}{\epsilon} \rceil + 1}^{N_{i,T}} \min \left\{ 1, \frac{\sigma T \sqrt{\log T}}{\epsilon^{3/2} j^{3/2}} \sqrt{6(3 + 8\epsilon^2)} \right\} \\
 &\leq K \left\lceil \frac{1}{\epsilon} \right\rceil + \sum_{i=1}^K \sum_{j=1}^{N_{i,T}} \min \left\{ 1, \frac{C}{j^{3/2}} \right\} \quad \text{where } C = \sigma T \sqrt{\log T} \epsilon^{-3/2} \sqrt{18 + 48\epsilon^2} \\
 &\leq K \left(\left\lceil \frac{1}{\epsilon} \right\rceil + j^* + \int_{j^*}^{\infty} C x^{-3/2} dx \right) \quad \text{with } j^* = \lceil C^{2/3} \rceil \\
 &= K \left(\left\lceil \frac{1}{\epsilon} \right\rceil + j^* + 2C(j^*)^{-1/2} \right) \\
 &\leq K \left\lceil \frac{1}{\epsilon} \right\rceil + 3KC^{2/3} \\
 &= K \left\lceil \frac{1}{\epsilon} \right\rceil + 3K \left(\sigma T \sqrt{\log T} \epsilon^{-3/2} \sqrt{18 + 48\epsilon^2} \right)^{2/3} \\
 &= K \left\lceil \frac{1}{\epsilon} \right\rceil + \frac{3K}{\epsilon} (\sigma T)^{2/3} (\log T)^{1/3} (18 + 48\epsilon^2)^{1/3}. \tag{73}
 \end{aligned}$$

Combining all results, we have:

$$\begin{aligned}
 Reg_{\mu}(\pi_{\epsilon}, T) &\leq \left(4 + \left\lceil \frac{1}{\epsilon} \right\rceil \right) K + \frac{(1 + 2^{1+q})KT^q}{2} \Upsilon_{\mu} \left(\left\lceil (1 - 2\epsilon) \frac{T}{K} \right\rceil, q \right) \\
 &\quad + \frac{3K}{\epsilon} (\sigma T)^{2/3} (\log T)^{1/3} (18 + 48\epsilon^2)^{1/3} \tag{74}
 \end{aligned}$$

□

D. Proof of Lemmas

Lemma D.1. For every arm $i \in [K]$, every time $t \in [T]$, and window width $1 \leq h_i \leq \frac{N_{i,t-1}}{2}$, we have:

$$\mathbb{P}(|\tilde{\mu}_i(t) - \bar{\mu}_i(t)| > \beta_i(t)) \leq 2t^{-2} \tag{75}$$

Proof. Firstly, we rewrite the equation as follows:

$$\mathbb{P}(|\tilde{\mu}_i(t) - \bar{\mu}_i(t)| > \beta_i(t)) = \mathbb{P}(\exists n \in [t-1] : |\tilde{\mu}_i(t)) - \bar{\mu}_i(t)| > \beta_i(t), N_{i,t-1} = n) \tag{76}$$

$$\leq \sum_{n=1}^{t-1} \mathbb{P}(|\tilde{\mu}_i(t) - \bar{\mu}_i(t)| > \beta_i(t), N_{i,t-1} = n). \tag{77}$$

Fixing n , we have:

$$h_i(t)(\tilde{\mu}_i(t) - \bar{\mu}_i(t)) \tag{78}$$

$$= \sum_{l=n-h_i+1}^n \left((X_i(l) - \mu_i(l)) + \frac{(T-t)}{2} \frac{(X_i(l) - \mu_i(l)) - (X_i(l-h_i) - \mu_i(l-h_i))}{h_i} \right) \tag{79}$$

$$= \sum_{l=n-h_i+1}^n \left(1 + \frac{(T-t)}{2h_i} \right) (X_i(l) - \mu_i(l)) - \sum_{l=n-h_i+1}^n \frac{(T-t)}{2} (X_i(l-h_i) - \mu_i(l-h_i)). \tag{80}$$

□

Since $X_i(l)$ is only drawn from $D_i(l)$, which only depends on l , all random variables $X_i(l)$ and $X_i(l-h_i)$ are independent. Also, since $\mathbb{E}[X_i(l)] = \mu_i(l)$, we can define $Z_i(l) := X_i(l) - \mu_i(l)$ and apply Azuma-Hoeffding inequality (Metelli et al.,

2022). For that, we compute the sum of square constants:

$$\sum_{l=n-h_i+1}^n \left[\left(1 + \frac{(T-t)}{2h_i} \right)^2 + \left(\frac{(T-t)}{2h_i} \right)^2 \right] \quad (81)$$

$$\leq \frac{h_i}{4h_i^2} \left[(2h_i + (T-t))^2 + (T-t)^2 \right] \quad (82)$$

$$\leq \frac{1}{4h_i} [3(T-t)^2 + 8h_i^2] , \quad (83)$$

where equation 83 holds since $(a+b)^2 \leq 2a^2 + 2b^2$. Thus, we have:

$$\mathbb{P}(|\tilde{\mu}_i(t) - \bar{\mu}_i(t)| > \beta_i(t)) \quad (84)$$

$$= \mathbb{P} \left(\left| \sum_{l=n-h_i+1}^n \left[\left(1 + \frac{(T-t)}{2h_i} \right) Z_i(l) - \frac{(T-t)}{2} Z_i(l-h_i) \right] \right| > h_i \beta_i(t) \right) \quad (85)$$

$$\leq 2 \exp \left(- \frac{(h_i \beta_i(t))^2}{2\sigma^2 \left(\frac{3(T-t)^2 + 8h_i^2}{4h_i} \right)} \right) \quad (86)$$

$$\leq 2t^{-3} . \quad (87)$$

Substituting this result into equation 77, we have:

$$\sum_{n=1}^{t-1} \mathbb{P}(|B_i(t) - \bar{\mu}_i(t)| > \beta_i(t), N_{i,t-1} = n) \leq \sum_{n=1}^{t-1} 2t^{-3} \leq 2t^{-2} , \quad (88)$$

which concludes the proof.

Lemma D.2. *For every arm $i \in [K]$, time $t \in [T]$ and any number of pulls $n \leq t$, we have:*

$$\mu_i(t) - \mu_i(n) - \frac{T-t}{2} \gamma_i(n-1) \leq \max \left(0, \frac{3t-2n-T}{2} \gamma_i \left(\frac{T-t}{2} \right) \right) \quad (89)$$

Proof. Firstly, we consider $t < n + \frac{T-t}{2}$. Then, we show that $\mu_i(t) - \mu_i(n) - \frac{T-t}{2} \gamma_i(n-1) \leq 0$.

$$\mu_i(t) \leq \mu_i \left(n + \frac{T-t}{2} \right) \quad (90)$$

$$\leq \mu_i(n) + \sum_{l=n}^{n+(T-t)/2-1} \gamma_i(l) \quad (91)$$

$$\leq \mu_i(n) + \frac{T-t}{2} \gamma_i(n-1) , \quad (92)$$

where equation 92 holds by concavity assumption (i.e., γ_i is non-increasing). Also, when $t < n + \frac{T-t}{2}$, we can easily see that $3t-2n-T \leq 0$, which completes our claim. Then, we consider the case when $t > n + \frac{T-t}{2}$. In this case, $3t-2n-T > 0$ is guaranteed. We decompose $\mu_i(t) - \mu_i(n)$ as follows:

$$\mu_i(t) - \mu_i(n) = \sum_{l=n}^{t-1} \gamma_i(n) \quad (93)$$

$$= \sum_{l=n}^{n+(T-t)/2-1} \gamma_i(n) + \sum_{l=n+(T-t)/2}^{t-1} \gamma_i(n) \quad (94)$$

$$\leq \frac{(T-t)}{2} \gamma_i(n) + \left(t - n - \frac{(T-t)}{2} \right) \gamma_i \left(n + \frac{(T-t)}{2} \right) \quad (95)$$

$$\leq \frac{(T-t)}{2} \gamma_i(n) + \left(\frac{3t-2n-T}{2} \right) \gamma_i \left(\frac{(T-t)}{2} \right) , \quad (96)$$

where equation 95 and equation 96 hold by concavity assumption, which completes proof. \square

E. Baselines

E.1. Description

- R-ed-UCB (Metelli et al., 2022) is a representative algorithm for the RMAB framework. It utilizes a derivative-based estimator to capture the growth rate of the reward function. By estimating this slope, the algorithm constructs an index designed to predict the instantaneous expected reward at the specific future time step.
- ET-SWGTS (Fiandri et al., 2025) is a Thompson Sampling-based algorithm adapted for RMAB framework. It addresses the non-stationary nature of reward growth by combining an initial exploration phase with a sliding-window mechanism. The algorithm first forces exploration to gather sufficient preliminary data for all arms. Subsequently, it updates the Gaussian posterior distributions using only the most recent observations within a fixed window, thereby forgetting outdated low rewards to track the current rising trend.
- TI-UCB (Xia et al., 2024) is tailored for the RMAB framework, specifically focusing on the "increasing-then-converging" reward trend. The core mechanism of the algorithm revolves around detecting the convergence point, where the critical moment when an arm's growth saturates and performance stabilizes. By focusing on identifying this transition to the asymptotic limit, TI-UCB aims to select the arm with the highest ultimate capacity.
- R-ed-AE (Amichay & Mansour, 2025) addresses the RMAB problem by specifically targeting environments where rewards exhibit linear drifts. The algorithm operates on a successive elimination principle, maintaining a set of active candidate arms. By estimating the growth parameters and future potential of each arm, R-ed-AE progressively discards arms that are statistically inferred to be suboptimal, thereby concentrating computational resources on identifying the most promising candidate.
- SW-UCB (Garivier & Moulines, 2011) is a modification of the standard UCB policy designed to handle non-stationary environments. It relies on a sliding window of fixed size to estimate the expected reward of each arm. By exclusively utilizing the most recent observations and discarding outdated history, the algorithm effectively forgets past behavior to adapt to dynamic changes in the reward distribution.
- SW-KL-UCB (Garivier & Cappé, 2011) enhances the sliding-window approach by replacing the standard Euclidean confidence interval with one based on KL divergence. While retaining the fixed-size window to track non-stationary changes, this modification allows for tighter confidence bounds, particularly in bounded reward settings, leading to more efficient exploration compared to the standard SW-UCB.
- SW-TS (Trovo et al., 2020) adapts the standard Thompson Sampling framework to non-stationary environments by incorporating a sliding-window mechanism. Instead of aggregating the entire history, the algorithm updates its Bayesian posterior distributions using exclusively the most recent observations contained within the window. This approach enables the probabilistic policy to track dynamic changes in the underlying reward distributions by effectively discarding outdated information.
- Rexp3 (Besbes et al., 2014) adapts the adversarial Exp3 algorithm to stochastic non-stationary settings by introducing a periodic restart mechanism. The algorithm divides the time horizon into fixed-size epochs and resets the Exp3 weights at the beginning of each epoch. This approach allows the policy to handle distribution changes by effectively limiting its memory to the current epoch, with the restart frequency typically tuned based on the total variation budget of the reward functions.
- Ser4 (Allesiardo et al., 2017) handles non-stationary environments by combining a successive elimination strategy with a periodic reset mechanism. Within each epoch, the algorithm progressively discards arms identified as suboptimal based on their estimated confidence bounds. To adapt to dynamic reward changes, Ser4 periodically resets the set of active arms, thereby "reviewing" previously eliminated candidates to check if they have become optimal in the new environment.

E.2. Hyperparameter

- R-ed-UCB: Confidence term $\delta = 0.001$, window size parameter $\epsilon = 1/4$ for synthetic experiment and $\epsilon = 1/32$ for online model selection.

- ET-SWGTS: For LTF setting, $\gamma = 1.0$, window size parameter $\tau = 1000$, forced exploration: $\Gamma = 10$. For Concave setting and online model selection, $\gamma = 1.0$, $\tau = 200$, $\Gamma = 1000$.
- TI-UCB: Confidence term $\delta = 0.01$, window size parameter $\omega = 100$, threshold $\gamma = 0.3$.
- R-ed-AE: Confidence term $\delta = 0.01$.
- SW-UCB: Sliding window term $\tau = 2\sqrt{T \log T}$, constant $\xi = 1.5$.
- SW-KL-UCB: $\tau = \sigma^{-4/5}$.
- SW-TS: $\beta = 0.5$, sliding window term $\tau = T^{1-\beta}$.
- Rexp3: $V_T = K$, $\gamma = \min \left\{ 1, \sqrt{K \log K / (e-1) \Delta_T} \right\}$, $\Delta_T = \lceil (K \log K)^{1/3} (T/V_T)^{2/3} \rceil$
- Ser4: $\delta = 1/T$, $\epsilon = 1/(KT)$, $\phi = \sqrt{N/TK \log(KT)}$.

F. Additional Experimental Results

In this section, we present supplementary experimental results to provide a comprehensive understanding of the algorithm's behavior. We analyze the pairwise win rates across random seeds, explicitly distinguishing between the Linear-Then-Flat (LTF) and Concave settings to highlight the specific advantages of CURE-UCB in each scenario.

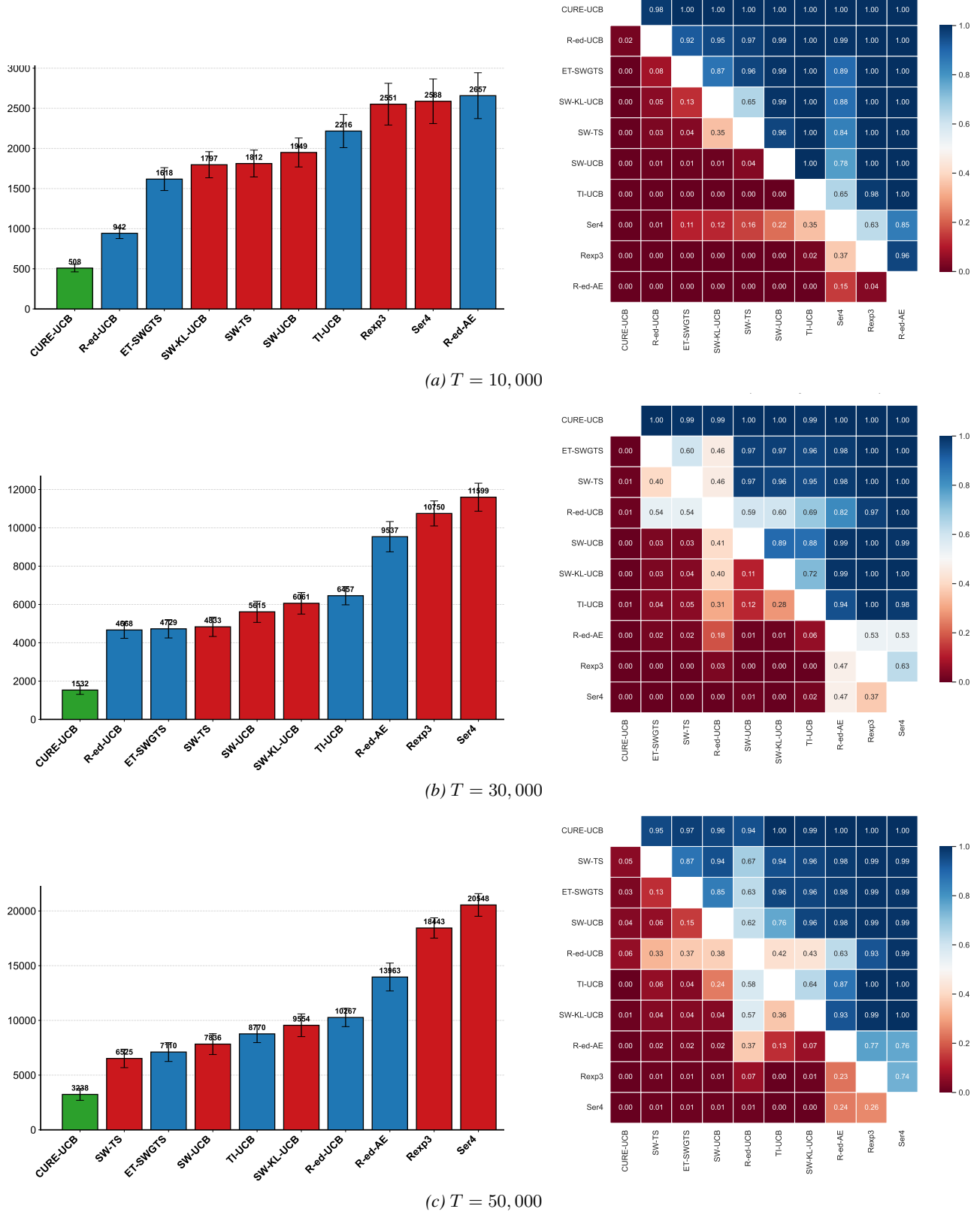


Figure 10. Additional experiment result for LTF setting (Left) Average Cumulative Regret with 95% confidence intervals, (Right) Pairwise Win Rate heatmap.

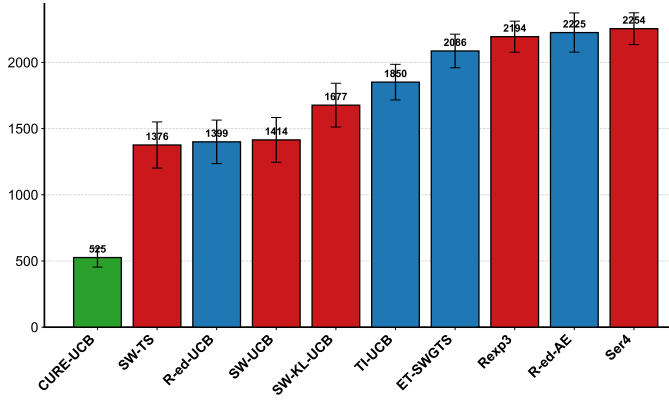
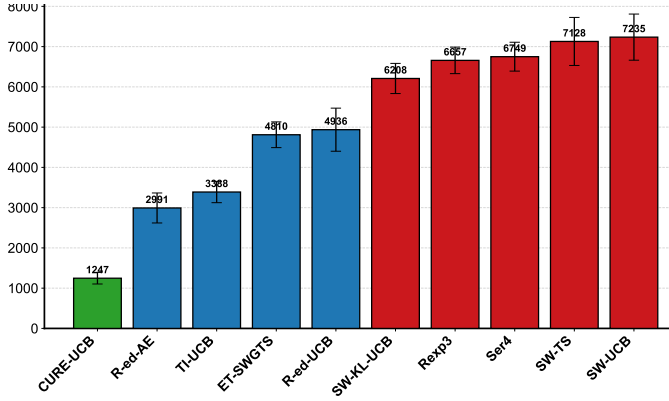
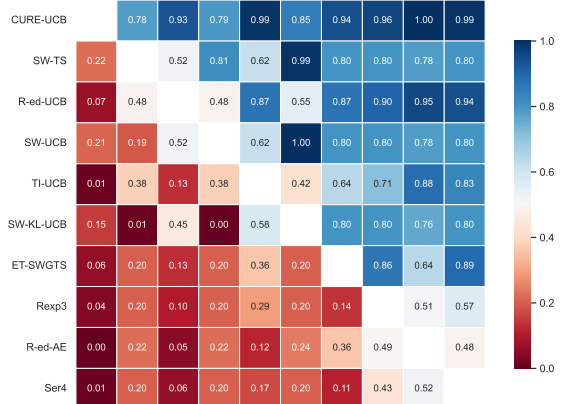
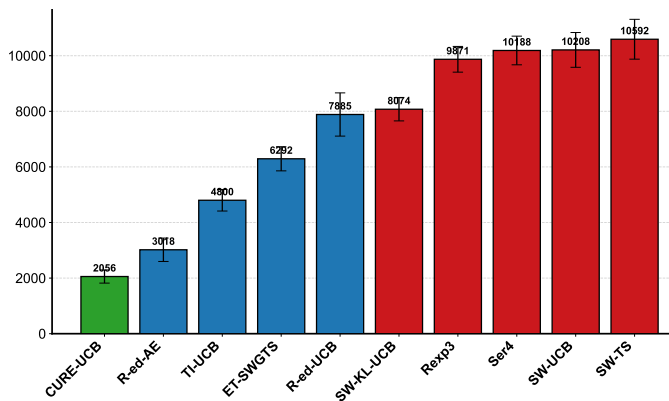
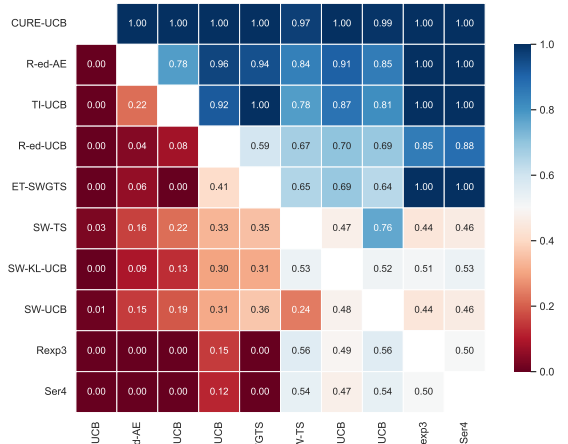
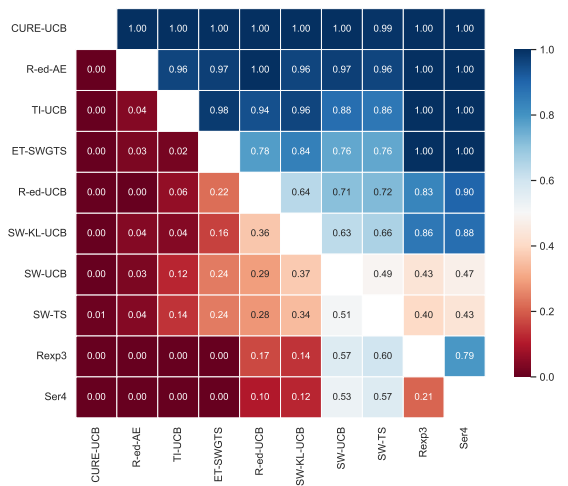

 (a) $T = 10,000$

 (b) $T = 30,000$

 (c) $T = 50,000$


Figure 11. Additional experiment result for Concave setting (Left) Average Cumulative Regret with 95% confidence intervals, (Right) Pairwise Win Rate heatmap.